

Received 1 November 2023, accepted 22 November 2023, date of publication 5 December 2023, date of current version 15 December 2023.

Digital Object Identifier 10.1109/ACCESS.2023.3339884

## RESEARCH ARTICLE

# Classifying the Vermicompost Production Stages Using Thermal Camera Data

ASMAA MOHAMED<sup>1,2</sup>, AHMED A. AKL<sup>3</sup>, M. M. BADR<sup>4</sup>, KHALIL AL RUQEISHI<sup>5</sup>, AHMAD SALAH<sup>1,6</sup>, AND AMR M. ABDELATIF<sup>1</sup>

<sup>1</sup>Faculty of Computers and Informatics, Zagazig University, Zagazig 35633, Egypt

<sup>2</sup>Department of Computer Science, High Institute for Management Sciences, Belqas 35511, Egypt

<sup>3</sup>Faculty of Computers and Information, Damanhour University, Damanhour 22511, Egypt

<sup>4</sup>Faculty of Agriculture, Zagazig University, Zagazig 44519, Egypt

<sup>5</sup>Department of Mathematical and Physical Sciences, College of Arts and Sciences, University of Nizwa, Nizwa 616, Oman

<sup>6</sup>College of Computing and Information Sciences, University of Technology and Applied Sciences, Ibri 516, Oman

Corresponding author: Ahmad Salah (ahmad@zu.edu.eg)

This work involved human subjects or animals in its research. Approval of all ethical and experimental procedures and protocols was granted by the European Union's Horizon 2020 Programme, under GA n° 817696.

**ABSTRACT** The procedure of processing the vermicompost production includes several stages, where the vermicompost material has different temperatures during these different stages. Thermal sensors play a key role in numerous fields, such as medical and agricultural applications. Thermal cameras can produce a thermal image or an array of values representing the array of sensory data. i.e., an array of temperatures. In this study, we proposed the first thermal imagery dataset of the vermicompost production process. The contributions of this work are two-fold using the proposed dataset. First, we framed the process of predicting the vermicompost production process as a classification problem. Second, we compared classifying the different stages of the process of vermicompost production based on two different input types, namely, thermal images and an array of temperatures. In other words, the classifier will be fed with an input (an image or an array of temperatures), and then the classifier will predict the vermicompost production stage. In this context, we utilized several machine and deep learning models as classifiers. For the utilized dataset, the study has been conducted on a set of images collected during the vermicompost production procedure which was collected every 14 days over 42 consecutive days, i.e., four classes. We proposed running a series of experiments to determine which input type yields better classification accuracy. The obtained results show that using thermal images for the sake of classifying the vermicompost production stages achieved higher accuracy, about 92%, in comparison to using the sensor array data, about 60%.

**INDEX TERMS** Classification, deep learning, machine learning, ResNet, SENet, sensor array, SVM, thermal images, vermicompost.

## I. INTRODUCTION

Thermal sensors are gadgets that gauge a system or area's temperature precisely. Temperature is a crucial physical measure related to all research branches. In reality, they make use of the Stefan-Boltzmann rule, which stipulates that every object emits thermal radiation in proportion to its temperature [1]. The non-visible electromagnetic spectrum is where the thermal sensor functions. In this context, thermal sensors can

provide a measurable means to define the material, whether it is a tangible object, the environment in which an object is placed, or the context in which an object is distributed. Sensors are classified in several ways by various researchers; one of them is thermal sensors [2].

Thermal imaging, also called InfraRed Thermography (IRT), is a term that literally translates as "beyond red" or "temperature picture". It is a method that uses a thermal camera for thermal data processing and acquiring thermal images [3]. There are two distinct measurement techniques that are used to analyze thermal camera images of body surfaces,

The associate editor coordinating the review of this manuscript and approving it for publication was Poki Chen<sup>1</sup>.

namely quantitative and qualitative IRT. Quantitative IRT is regarded as more complicated to analyze than qualitative IRT. The former technology enables the traditional visualization of thermal patterns and quantification of surface temperatures and their differences. Temperature calibration should be carried out by detecting surfaces or objects with known fixed temperatures. A radiometric temperature reading is necessary to be able to compare results with defined restrictions and keep track of even little deviations. On the other hand, qualitative IRT does not require knowing the temperature values to recognize issues. It is very simple to identify deviations from the norm [4], [5].

Thermal imaging data is easily collected in real-time from a variety of platforms, such as the sea, air vehicles, and land. As a result of their vital importance, the use of thermal cameras has spread in recent times in different fields, e.g., medical, industrial, and agricultural. The main focus of this paper is a thermal imaging application in agriculture. Thermal imaging can be applied to various agricultural tasks, such as planning irrigation [6], estimating soil water status, estimating crop water stress [7], [8], evaluating the viability of seedlings [9], determining the maturity of fruits and vegetables [10], [11], identifying fruits with bruises [12], and identifying plants with disease and pathogens [13], [14]. Many publications have explored the possible applications of thermal imaging in agriculture and the food business [9], [15], [16]. Despite these efforts, we did not find any literary evidence proposing the use of thermal imaging analysis in vermicompost production. This finding motivated this research to contribute the first method that utilizes thermal imaging in the analysis of vermicompost.

The proposed work framed the task of vermicompost production stages as a classification problem. The image classification problem is a solved problem with a high accuracy while the progress of tabular data classification is still much less accurate relative to the image classification. Thus, we preferred to handle the task of vermicompost production stages as an image classification problem over a tabular data classification problem. In the proposed study, we extended these efforts, of using thermal cameras in the agricultural field, to utilize thermal imaging in classifying the different stages of the vermicompost production procedure. To achieve this goal, we collected the temperatures of the mixture of soil and animal waste, which is used to produce vermicompost, at four different stages using a thermal camera. Then, we saved the collected data from the thermal camera as a collection of images in one dataset and a collection of sensor array data (i.e., temperature values) in another dataset. Finally, different deep learning (DL) and machine learning (ML) classifiers were trained on the two types of thermal datasets separately to figure out which type of thermal dataset is easier to classify.

The list of contributions can be listed as follows:

- 1) To our knowledge, we provided the first thermal imagery dataset of the process of vermicompost

fertilizer production stages. The dataset is publicly available on GitHub<sup>1</sup>

- 2) To our knowledge, this is the first study to frame the problem of predicting the process of vermicompost fertilizer production stages based on thermal images as a classification problem.
- 3) To our knowledge, this is the first study to compare the prediction accuracy based on the two types of thermal data, namely, thermal images and sensory array data.
- 4) The comparison is based on thermal data collected during the vermicompost production stages. Several machines and deep learning models were utilized to figure out which type of thermal data could be used to train the model and achieve higher accuracy.

The remainder of this paper is structured as follows: Section II reviews the background and related work. Section III describes the suggested technique. Section IV discusses the experimental findings. Finally, Section V wraps up the work and discusses future plans.

## II. BACKGROUND

A thermal imaging camera features a sensitive heat sensor that can pick up on the smallest temperature variations from nearby objects. After gathering this radiation data from the items, the device uses temperature differential data to display their temperature in a digital radiometric image. Fig. 1 illustrates the infrared camera's anatomy. The primary components of an infrared camera are lenses, detectors, image processing circuits, and user interface control. The IR camera works by concentrating the collected IR waves on the detector through the lens. The IR-sensitive components of the detector are organized in an array known as the focal plane array. These IR-sensitive elements are very small. The number of elements in the array influences the resolution of the camera's IR images [17], [18]. Then, the signal processor module extracts the electronic signals from the detector and displays them either as an array of values or by mapping these values to a colored bitmap image.

The infrared camera can be mounted on various supports to gather thermal images as well. For neighborhood-scale design research, it is mounted on a rooftop observatory [19]; for micro-scale studies, it is used with a tripod, portable device, or smartphone [20]; and for studies spanning the neighborhood scale and building scale, it is mounted on a drone [21]. As a result, several airborne and satellite thermal sensors have been created and are currently being employed directly or indirectly for numerous agricultural applications.

## III. METHODOLOGY

### A. OVERVIEW

Fig. 2 depicts the overview of the proposed methodology. As shown in Fig. 2, we proposed collecting two types of datasets of the vermicompost production process using a

<sup>1</sup>[https://github.com/AhmedAAkl/vermicomposit\\_stages\\_prediction](https://github.com/AhmedAAkl/vermicomposit_stages_prediction)

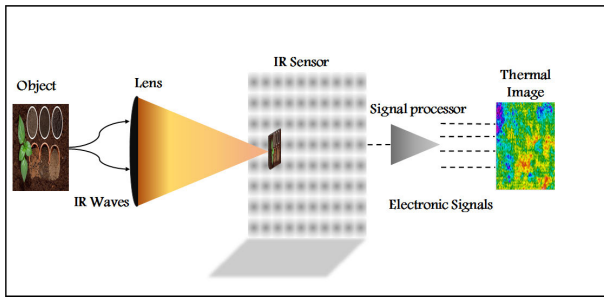


FIGURE 1. The design of the infrared camera.

thermal camera. The first dataset includes thermal images while the second dataset includes an array of temperature values (i.e., real numbers) instead of each image. Then, we proposed using different deep learning models for the purpose of feature extraction and a machine learning model for classification purposes where the two datasets were treated independently. Finally, the dataset that helps to achieve the highest accuracy is reported based on the best evaluation metric values.

## B. DATASET COLLECTION

The experiment was carried out for 42 consecutive days at the Agricultural Engineering Department, Faculty of Agriculture at Zagazig University, Egypt, according to the produce methods and technology in full compliance with the European Union's Horizon 2020 Programme, under GA n° 817696. During this period, 1,869 thermal images were required; these images were captured with a pocket thermal camera, model PTi120, Fluke.

The vermicomposting production unit was set up in plastic bins of dimensions (60 × 40 × 30 cm), using red earthworms (*Eisenia fetida*) to be used for producing vermicomposting rates (350 to 360 worms per m<sup>3</sup> of bed volume). The bottom of the bin is inclined to drain the excess water from vermicompost units, with a small sump being put in to collect the drain water. The starter was prepared from cow dung and biogas slurry during the composting process, where it was used as feeding material to breed sufficient numbers of earthworms. To attain the required worm population, basic material sources of organic waste are provided during vermicomposting production. Biodegradable waste (weed biomass, vegetable and fruit waste, leaf litter) were used as basic raw materials to enrich the quality of vermicompost. Bedding material provides the worms with a stable habitat and feeds them with agricultural waste. Under constant operating conditions, maintaining the adequate moisture content of 70% ± 2, aeration, 7 pH, and temperature of 30 °C ± 2 during the composting period. Preparing vermicompost material includes the following phases:

1. In the first step, the process involves waste material collection, pre-digestion to waste, earthworm bed preparation and composting, vermicompost earthworm harvesting, and vermicompost packing and storage.

2. Once the waste has been collected, it is shredded to break it down into smaller bits. By mechanically eliminating foreign items, only organic waste is left for subsequent processing. Finally, organic waste is kept in proper containers.

3. The organic waste is then in the pre-digestion process for seven days by steeping the materials and cattle dung slurry, and the organic waste becomes more easily decomposable, making it suitable for earthworms to consume. This method helps accelerate the breakdown of the waste and enhances nutrient availability for plants when used as fertilizer.

4. Constructing the earthworm bed, we kept a 20cm layer of chopped dry leaves/grasses as bedding material at the bottom of the bed. This material will provide a comfortable environment for the earthworms to thrive.

5. Beds of partially decomposed material of specific dimensions (60 × 40 × 20 cm) were made. Each bin contains 6kg of raw material and a starter.

6. Red earthworms (250g per bin) were released in the bed's upper layer, with water sprinkled to maintain a 70% moisture content.

7. The bins were kept moist by a sprinkling of water daily and covered with gunny bags, stirred once after 15 days, and the finished product weighs 65-75% of the raw materials used.

8. Thermal images were collected every two weeks and the collected data can be saved as an RGB image and as an array of temperature values; one dataset is image-based and the other is a numerical dataset. To capture the temperature of the soil (i.e., vermicompost material), a thermal camera, Fluke PTi120,<sup>2</sup> is utilized. The saved images were converted to the RGB format using the *high contrast* color palette; the *high contrast* color palette is a standard implemented in most of the commercial thermal cameras.<sup>3,4</sup>

## C. PREPROCESSING

The collected datasets are of two different types, i.e., images and numerical data. Both of them are generated using a thermal camera. The spatial resolution of the utilized thermal camera is 90 × 120 pixel detectors IR-Fusion, i.e., real numbers. These values can be saved as an array of temperature values or as an RGB image. For the imagery dataset, as the images have different sizes, we pre-processed the thermal images by resizing them to 224 × 224 × 3 pixels to meet the input form of the model. In addition, to speed up the training process we normalized their values into a range between (0,1). On the other hand, we pre-processed the thermal sensory data to convert the array of temperature values into grayscale images, as it consists of one channel. Then, we resized the converted grayscale images into 90 × 90 × 1 pixels. Finally, we normalized the thermal numerical arrays into a range between 0 and 1. Thus, both the datasets

<sup>2</sup><https://www.fluke.com/en/product/thermal-cameras/pocket-pti120>

<sup>3</sup><https://www.flir.com/discover/industrial/picking-a-thermal-color-palette/>

<sup>4</sup><https://www.fluke.com/en/learn/blog/thermal-imaging/how-color-palettes-alarms-and-markers-improve-infrared-inspections>

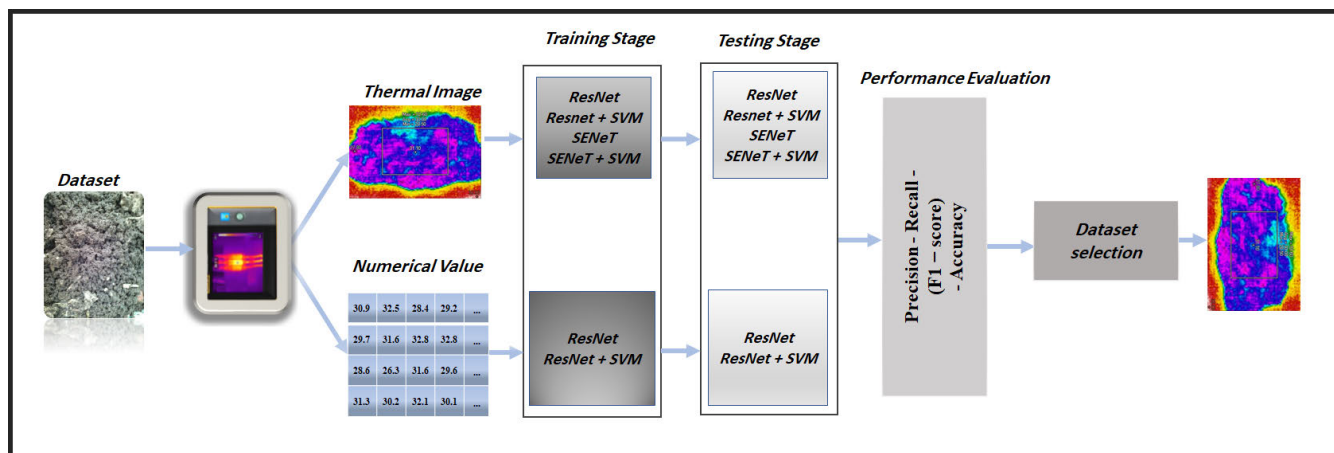


FIGURE 2. Flow diagram of the proposed method.

are normalized into a range between 0 and 1 and both can be treated as images.

#### D. FEATURE EXTRACTION

We proposed using two transfer learning models for the sake of feature extraction, namely, the Residual Network (ResNet) and the Squeeze-and-Excitation Network (SENet). In the following text, a justification for selecting these two models is outlined and then an amendment of these two models will be exposed to be used as feature extraction models instead of classifier models.

ResNet was introduced by He Kaiming’s model in 2015 [22]. The 2015 ILSVRC and COCO competitions’ ImageNet Detection, ImageNet Localization, COCO Detection, and COCO Segmentation tasks were won by this model. ResNet is constructed using layers with variable counts, such as 34, 50, 101, 152, and even 1,202. As deep learning training often takes a lot of time and is only capable of training a limited number of layers, this architecture was developed to solve these challenges. The ResNets model has a significant advantage over other architectural models in that its performance is unaffected by the depth of the architecture. Down-sampling and its limited ability to capture multi-scale features are its main shortcomings.

SENet is the winner of the ILSVRC 2017 competition, [23]. It is a distinct architectural, Squeeze, and excitation unit that was created to improve neural network performance. The SE block undertakes positive channel-wise feature re-calibration while suppressing less valuable features. SENet’s structures are commonly used in a variety of tasks and have demonstrated genuine performance improvements. The two main phases of the SE block are squeezing and excitement. Squeezing produces the channel description and is dependent on global average pooling. The gating arrangement for the excitation section is simple and uses a sigmoid activation function. The result is a scalar that

has been channel-wise amplified by the feature map. [24]. By learning, a SENet architecture can automatically determine the significance of each feature channel. In accordance with this significance, the features that are useful for classification are enhanced, while those that are less useful are suppressed. The classification performance of thermal images can be significantly improved by the weighted feature.

As both the ResNet and SENet models are proposed as classifier models, we proposed replacing the last layer (i.e., the classification layer) with a fully connected (FC) layer of size 128. Thus, the input image pixels were used as an input and then the transfer learning model (i.e., ResNet and SENet) extracted the 128 most significant features. In other words, the added FC layer extracts the important features of each input image and then these extracted features will be used as inputs to the classifier models, as depicted in Fig. 3.

#### E. CLASSIFICATION

The main idea of the proposed work is to predict vermicompost production stages based on the collected thermal images. Thus, the problem is framed as a multiclass classification problem where each class represents a different stage of the vermicompost production stages, as shown in Fig. 2. In this subsection, a detailed elaboration is provided for the classification task.

For the classification task, we proposed utilizing an SVM model [25] and a transfer deep learning (i.e., ResNet). The SVM model is a machine learning technique that makes use of statistical learning theory; it reduces the upper bound of the model generalization error while minimizing sample error. It incorporates structural risk reduction criteria, which improves the generalizability of the model. The core concept behind SVM would be to use the kernel transform to accurately classify low-dimensional, linearly indivisible

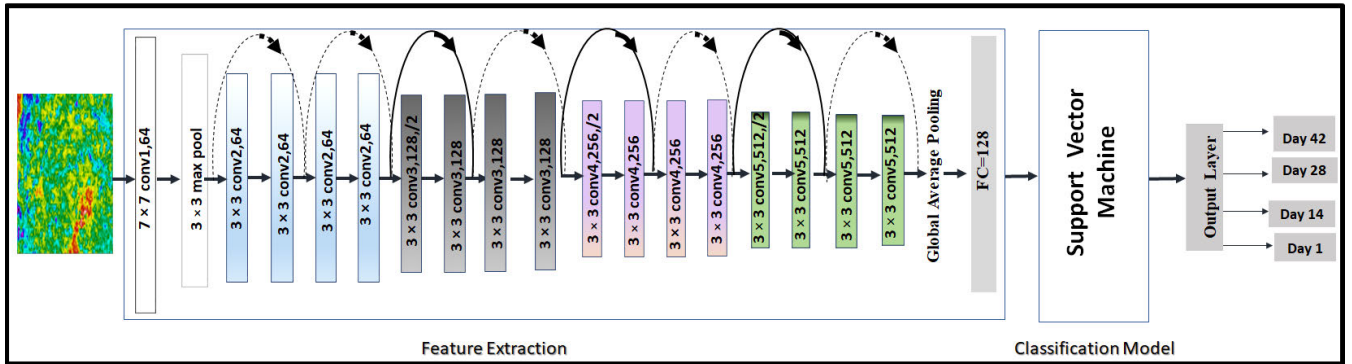


FIGURE 3. The proposed model architecture is a combination of a deep neural network (feature extraction) and an SVM model (classification).

problems in high-order space. SVM is frequently employed in the classification of remote sensing data [26], [27].

In the model training phase, we used the two datasets independently and split them into training and testing subsets, 80% for training and 20% for testing. Next, we trained the utilized models and tested these models on the test dataset. Then, we evaluated the performance of the proposed methods using different evaluation metrics, e.g., precision.

#### F. IMPLEMENTATION DETAILS

To complete the proposed study, we chose machine learning on both thermal imaging and thermal numerical array datasets, to carry out the proposed study since it is cutting-edge technology that can be utilized to address practically any problem, whether it is classification or object detection, in almost any area. Following data collection, the thermal images and thermal numerical arrays were pre-processed to remove temperature scales and other markings and then resized to  $224 \times 224 \times 3$  and  $90 \times 90 \times 1$  respectively. For all the experiments, we utilized a reduction learning rate on a plateau (RLRP) which is another callback function that automatically lowers the learning rate after a certain specified value depending on the relative increase in the model's performance [28].

We checked the validation loss with a factor of 0.2 and a minimal delta of 0.000001 with a patience value equal to five. We used the early stop technique to discontinue training at the right time and avoid the overfitting problem with a value of 20. Thus, the process of training the proposed model stopped when the accuracy did not improve for 20 successive epochs. For training, the batch size we utilized was 32 and the Adam optimizer is used as an optimizer with a compilation-based sparse categorical cross-entropy loss function to our model. In an experimental study, Kingma and Ba [29] demonstrated that the Adam optimizer is the fastest optimizer relative to the most well-liked gradient descent optimization technique. We utilized popular neural network frameworks such as TensorFlow, Caffe, and CNTK.

#### G. EVALUATION METRICS

The metrics that are used for evaluating the performance of the classifier model can be defined as follows: TP (True Positive) which means that the classifier correctly predicts that the soil is positively fertilized. The precision metric can be computed as the true positive (TP) divided by the total positive cases ( $TP + FP$ ) as shown in Equation 1.

$$Precision = \frac{TP}{TP + FP} \quad (1)$$

The recall metric is computed as the division of TP over the total correct predictions ( $TP + FN$ ). This is shown in Equation 2.

$$Recall = \frac{TP}{TP + FN} \quad (2)$$

The F1-score metric can be computed as the harmonic mean between the precision and the recall as shown in Equation 3.

$$F1 - score = \frac{TP}{TP + 0.5(FP + FN)} \quad (3)$$

The accuracy metric is computed as the ratio between the correct prediction outcomes and the total prediction outcomes as shown in Equation 4.

$$Accuracy = \frac{TP + TN}{TP + TN + FP + FN} \quad (4)$$

The confusion matrix is a well-known metric, also known as the UT error matrix, It may be used for both binary classification and multi-class classification issues, and it is the table that describes how a classification model performs on a set of test data.

## IV. EXPERIMENTAL RESULTS

### A. SETUP

To design the proposed models, we built an environment using the Python programming language version 3.9.16 on a computer with a Linux Operating System. This machine

has a Dual Core Processor Intel(R) Core(TM) of 2.50 GHz, 24 GB of system RAM, and Nvidia T4 with 16 GB of RAM. Then, we proposed dividing the utilized dataset into three subsets: the training, the validation, and the testing sets. We used the training and validation sets to train the model, and the test set—which is not visible during training—was used to test it. This training strategy fixes the overfitting issue and improves the model's generalizability. Also, we used Early Stopping and decreased Learning Rate On the Plateau during the training procedure. These two methods made it easier to complete the task of generalization. TensorFlow 2.5, a well-known deep learning framework, was used to create all of the suggested deep learning models. The proposed code and dataset are available on GitHub<sup>5</sup> for the sake of results reproducibility.

Two examples of the thermal images and array of thermal sensory data are depicted in Fig. 4, where sensor readings along with the corresponding temperature within the array are presented in Fig. 4a. The image in Fig. 4b depicts an example of a thermal image taken by thermal cameras. Thermal images are very sensitive heat sensors that can detect even small temperature variations such values in the left figure. Once the data from the infrared radiations generated by the object has been collected, a map-out thermal picture based on the variations and inflections of the temperature values. Millions of detector pixels are stacked in a grid in this array. The infrared radiation concentrated on each sensor array pixel causes it to respond by emitting an electrical signal. The camera processor receives this electrical signal and processes it mathematically to provide a color map of the object's observed temperature as shown in Fig. 4b the resultant color matrix is delivered to the camera's memory, and a separate color channel is given to each temperature value. Typically, these created pictures are grayscale. White items are hot and black objects are cold, with gray indicating a degree between the two. However, the newer and more sophisticated thermal imaging camera types may produce more colors, employing a color spectrum of yellow, orange, purple, red, and blue, to assist users in detecting other factors within the output image.

## B. RESULTS AND DISCUSSION

We conducted a set of experiments to investigate the performance of the utilized models for both the classification and feature extraction tasks. The comparison criteria are based on four evaluation metrics, namely, precision, recall, F1-score, and accuracy. The results include numerical values of the evaluation metrics, the visual results of the confusion matrices, underfitting analysis, cross-validation analysis, and the confidence interval analysis to outline the proposed model's level of trust. The main goal of these experiments is to evaluate the accuracy of classifying the thermal images of different vermicompost production stages. Besides, the

experiments reveal the performance gap between classifying thermal images generated by the built-in thermal camera color palette against the numerical values representing the temperature values.

In the first set of results, we reported the numerical values of the four evaluation metrics in Table 1. These results are for both datasets, thermal image, and thermal numerical values. In Table 1, it is obvious that the models trained on the thermal images achieved better results relative to the models trained on the sensor array values, i.e., sensors' numerical values. For the thermal images dataset, three different models were utilized for the classification purpose. The first model is a pre-trained deep learning model (i.e., SENet model) which achieved 89.84%. The second model consists of a deep learning model for feature extraction, i.e., SENet, and an SVM model for classification purposes which achieved an accuracy rate of 90.09%; we called this model SENet+SVM. The third model utilizes the ResNet model, which is a pre-trained deep learning model, for feature extraction and an SVM model for classification purposes; we called this model ResNet+SVM. The proposed ResNet+SVM achieved the highest accuracy rate, 92.24%, as listed in Table 1.

In contrast, for the sensor array values dataset (i.e., temperature values), we trained two models on the sensor array data. The first model is the pre-trained deep learning model ResNet which achieved a 59.89% accuracy rate. The second model consists of a deep learning model for feature extraction, i.e., ResNet, and an SVM model for classification which achieved a 59.63% accuracy rate as well. The SENet was not able to run on this dataset, as the image represents the sensor array data consisting of one channel whereas the SENet model requires an input with three channels. Thus, the results of Table 1 indicate that using the thermal images for training is the preference over the sensor array data for the task of classifying the vermicompost production stages. The first research question of this work was answered with the results of Table 1. For all of the four evaluation metrics, the image-based dataset was easier to predict relative to the thermal values dataset. The performance gap of the predictive models was about 30% on average. Thus, the recommendation based on the obtained results is to use the thermal images for classification purposes. These results emphasize that using the color palette provider by the thermal camera, i.e., Fluke PTi120, provided an easier dataset to be classified relative to converting the numerical values, i.e., temperature values, into images.

As the ResNet+SVM model achieved the best results, this model's performance analysis is detailed in the following text. As the problem at hand is a multi-class problem, the accuracy of each class out of the existing four classes, the vermicompost production stages, are depicted as a heatmap in Fig. 5 where the values are obtained from the confusion matrix. Evidently, the accuracy of predicting the images of each class varied. Last week's, i.e., day 42, class was the most

<sup>5</sup>[https://github.com/AhmedAAkl/vermicomposit\\_stages\\_prediction](https://github.com/AhmedAAkl/vermicomposit_stages_prediction)

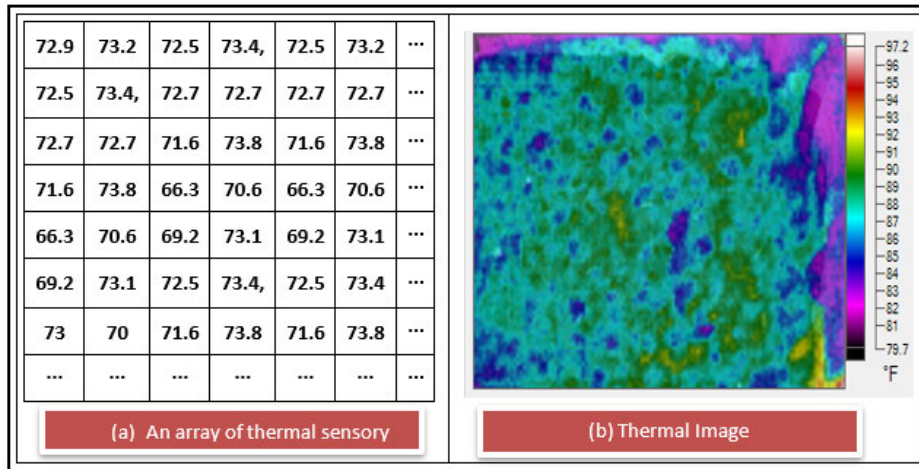


FIGURE 4. Sample of an array of thermal sensory data and thermal images.

TABLE 1. The evaluation metric scores the proposed classifier models trained on either the thermal images or thermal numerical data.

	Model	Precision	Recall	F1-score	Accuracy
Thermal Images	SENet (Transfer Learning)	91.00%	90.00%	89.83%	89.84%
	SENet (Feature Extraction) + SVM	91.00%	91.00%	90.09%	90.09%
	<b>ResNet (Feature Extraction) + SVM*</b>	<b>92.00%</b>	<b>92.00%</b>	<b>92.24%</b>	<b>92.24%</b>
Thermal Numerical Values	ResNet (Transfer Learning)	60.00%	60.00%	59.89%	59.89%
	ResNet + SVM	60.00%	60.00%	59.89%	59.63%

\*Bold values represent the best results.

challenging task, as the accuracy rate for predicting this class was 84%.

The second point of analysis of the ResNet+SVM model is the feature extraction quality. We proposed evaluating whether the ResNet model used in the feature extraction task was suffering from overfitting or underfitting problems. Thus, we depicted the train and test scores for both accuracy and loss metrics as in Fig. 6. Fig. 6a shows a very close accuracy rate for the training and test sets and Fig. 6b shows very close loss rates for the training and test sets. Thus, the ResNet utilized for the feature extraction did not suffer from either the overfitting or underfitting problems.

To analyze the proposed model accuracy variance, we performed the cross-validation test alongside the confidence interval analysis, as the third point of analysis. We performed this analysis on the best-performing model, i.e., the ResNet+SVM classifier. The ResNet+SVM was run on 10 different folds, i.e.,  $k = 10$ . Then, we used the cross-validation results to evaluate the trust level of the proposed ResNet+SVM with the 95% confidence interval. Fig. 7 depicts the error margin with a 95% confidence interval. In Fig. 7, regardless of the  $k$  value used, the error

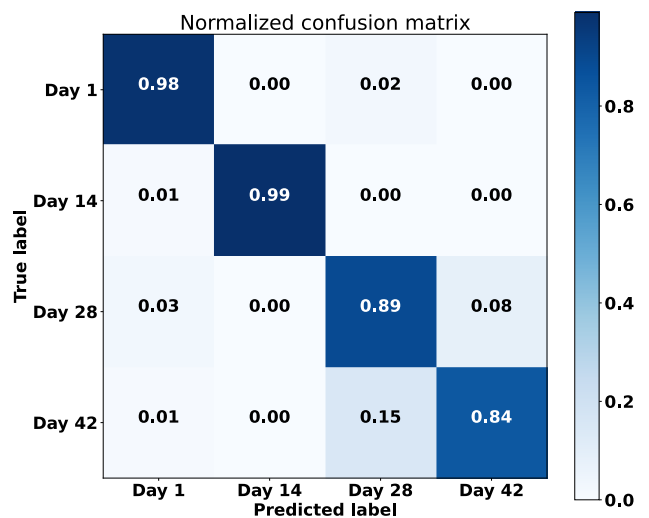


FIGURE 5. Confusion matrix for the proposed ResNet+SVM classifier.

margin was still narrow. The narrow depicted error margin in Fig. 7 reflects a high trust level of the classification accuracy results.

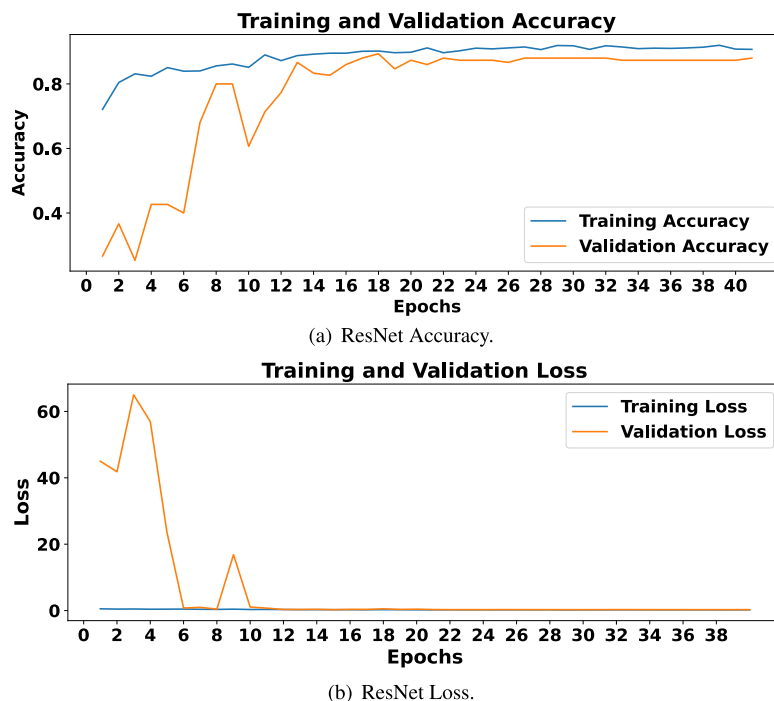


FIGURE 6. Evaluation metrics of tuned ResNet architecture (a) Training and test accuracy (b) Training and test loss.

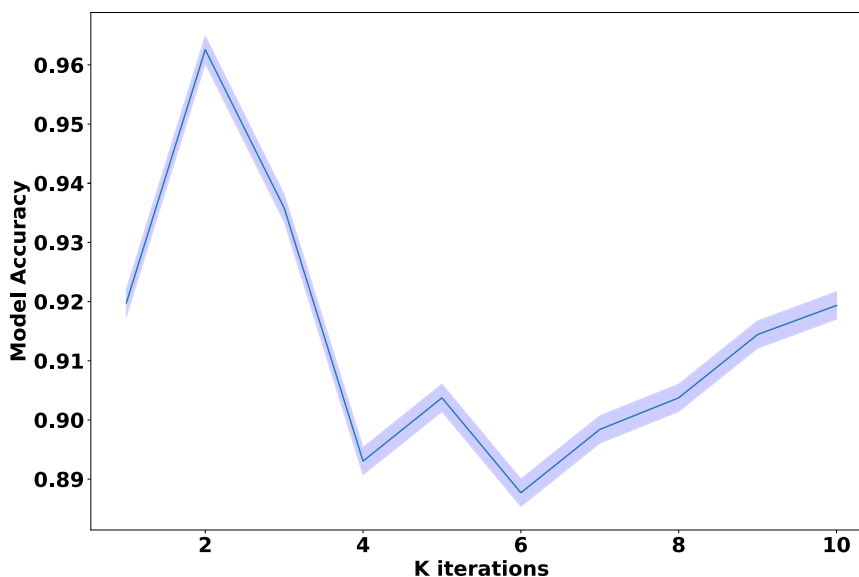


FIGURE 7. The proposed ResNet+SVM model's accuracy with 95% confidence interval for 10 cross-validation folds.

Finally, the ResNet+SVM classifier was run 10 times to measure the prediction time. Given the input image to the proposed ResNet+SVM classifier, the average prediction time was 30.4 milliseconds and the standard deviation was 2.6 milliseconds. This reported time reflects the real-time property of the proposed predictive model.

### V. CONCLUSION

The thermal cameras were successfully utilized in different fields for different purposes. Thermal cameras can produce two types of data, namely, 1) thermal images and 2) sensor array data (i.e., an array of temperature values). In this work, we proposed to utilize these advancements in thermal



cameras to classify the vermicompost production stages. Thus, we collected the first thermal dataset for the vermicompost fertilizer production stages, as per our knowledge. The collected dataset consists of four classes that represent the four stages of the vermicompost production procedure, where the thermal data were collected as thermal images and sensor array data. Then, we trained a set of machine and deep learning models on the two thermal data types separately. Besides, we proposed investigating which thermal data type, out of these two types, can be easier to use for the predictive tasks. The obtained results show that training predictive models on the thermal images can achieve better results in comparison to training them on sensor data. The performance gap for the accuracy metric is about 30%. The proposed trained model is able to predict the vermicompost production stage for the given thermal data within 30 milliseconds on average. The future direction is to improve the classification results by proposing a new CNN-based architecture and then train it on the thermal image dataset from scratch, instead of using transfer learning.

#### DATA AVAILABILITY

The dataset is publicly available.<sup>6</sup>

#### CONFLICTS OF INTEREST

The authors declare no conflict of interest.

#### REFERENCES

- [1] A. Prakash, "Thermal remote sensing: Concepts, issues and applications," *Int. Arch. Photogramm. Remote Sens.*, vol. 33, pp. 239–243, Jan. 2000.
- [2] M. Javaid, A. Haleem, S. Rab, R. P. Singh, and R. Suman, "Sensors for daily life: A review," *Sensors Int.*, vol. 2, 2021, Art. no. 100121.
- [3] R. Usamentiaga, P. Venegas, J. Guerediaga, L. Vega, J. Molleda, and F. Bulnes, "Infrared thermography for temperature measurement and non-destructive testing," *Sensors*, vol. 14, no. 7, pp. 12305–12348, Jul. 2014.
- [4] E. Barreira, R. M. S. F. Almeida, M. L. Simões, and D. Rebelo, "Quantitative infrared thermography to evaluate the humidification of lightweight concrete," *Sensors*, vol. 20, no. 6, p. 1664, Mar. 2020.
- [5] A. Kirimat, O. Krejcar, and A. Selamat, "A mini-review of biomedical infrared thermography (B-IRT)," in *Bioinformatics and Biomedical Engineering*. Granada, Spain: Springer, 2019, pp. 99–110.
- [6] G. Singh, D. Sharma, A. Goap, S. Sehgal, A. K. Shukla, and S. Kumar, "Machine learning based soil moisture prediction for Internet of Things based smart irrigation system," in *Proc. 5th Int. Conf. Signal Process., Comput. Control (ISPCC)*, Oct. 2019, pp. 175–180.
- [7] C. Pradawet, N. Khongdee, W. Pansak, W. Spreer, T. Hilger, and G. Cadisch, "Thermal imaging for assessment of maize water stress and yield prediction under drought conditions," *J. Agronomy Crop Sci.*, vol. 209, no. 1, pp. 56–70, Feb. 2023.
- [8] J. Xu, Y. Lv, X. Liu, T. Dalson, S. Yang, and J. Wu, "Diagnosing crop water stress of rice using infra-red thermal imager under water deficit condition," *Int. J. Agricult. Biol.*, vol. 18, no. 3, pp. 565–572, Jun. 2016.
- [9] G. ElMasry, R. ElGamal, N. Mandour, P. Gou, S. Al-Rejaie, E. Belin, and D. Rousseau, "Emerging thermal imaging techniques for seed quality evaluation: Principles and applications," *Food Res. Int.*, vol. 131, May 2020, Art. no. 109025.
- [10] A. Hussain, H. Pu, and D.-W. Sun, "Innovative nondestructive imaging techniques for ripening and maturity of fruits—A review of recent applications," *Trends Food Sci. Technol.*, vol. 72, pp. 144–152, Feb. 2018.
- [11] P. Pathmanaban, B. K. Gnanavel, and S. S. Anandan, "Recent application of imaging techniques for fruit quality assessment," *Trends Food Sci. Technol.*, vol. 94, pp. 32–42, Dec. 2019.
- [12] Y. Dong, Y. Huang, B. Xu, B. Li, and B. Guo, "Bruise detection and classification in jujube using thermal imaging and DenseNet," *J. Food Process Eng.*, vol. 45, no. 3, p. e13981, Mar. 2022.
- [13] M. Stoll, H. R. Schultz, G. Baecker, and B. Berkelmann-Loehnertz, "Early pathogen detection under different water status and the assessment of spray application in vineyards through the use of thermal imagery," *Precis. Agricult.*, vol. 9, no. 6, pp. 407–417, Dec. 2008.
- [14] A. Danno, M. Miyazato, and E. Ishiguro, "Quality evaluation of agricultural products by infrared imaging method," *Mem. Fac. Agr. Kagoshima Univ.*, vol. 16, pp. 157–164, Aug. 1980. [Online]. Available: <https://ir.kagoshima-u.ac.jp/record/412/files/KJ00000010823.pdf>
- [15] M. Mohd Ali, N. Hashim, S. A. Aziz, and O. Lasekan, "Emerging non-destructive thermal imaging technique coupled with chemometrics on quality and safety inspection in food and agriculture," *Trends Food Sci. Technol.*, vol. 105, pp. 176–185, Nov. 2020.
- [16] C. P. Weatherspoon and R. J. Laacke, "Infrared thermography for assessing seedling condition: Rationale and preliminary observations," *Tech. Rep.*, 1985. [Online]. Available: <https://www.scirp.org/reference/referencespapers?referenceid=1300609>
- [17] A. Rogalski, "Infrared detectors: An overview," *Infr. Phys. Technol.*, vol. 43, nos. 3–5, pp. 187–210, Jun. 2002.
- [18] G. Messina and G. Modica, "Applications of UAV thermal imagery in precision agriculture: State of the art and future research outlook," *Remote Sens.*, vol. 12, no. 9, p. 1491, May 2020.
- [19] M. Martin, V. Ramani, and C. Miller, "InfraRed investigation in Singapore (IRIS) observatory: Urban heat island contributors and mitigators analysis using neighborhood-scale thermal imaging," 2022, *arXiv:2210.11663*.
- [20] J. Ma, P. Shang, C. Lu, S. Meraghni, K. Benaggoune, J. Zuluaga, N. Zerhouni, C. Devalland, and Z. Al Masry, "A portable breast cancer detection system based on smartphone with infrared camera," *Vibroengineering Proc.*, vol. 26, pp. 57–63, Sep. 2019.
- [21] T. Rakha, A. Liberty, A. Gorodetsky, B. Kakilioglu, and S. Velipasalar, "Heat mapping drones: An autonomous computer-vision-based procedure for building envelope inspection using unmanned aerial systems (UAS)," *Technol. Archit. + Des.*, vol. 2, no. 1, pp. 30–44, Jan. 2018.
- [22] K. He, X. Zhang, S. Ren, and J. Sun, "Deep residual learning for image recognition," in *Proc. IEEE Conf. Comput. Vis. Pattern Recognit. (CVPR)*, Jun. 2016, pp. 770–778.
- [23] J. Hu, L. Shen, and G. Sun, "Squeeze-and-Excitation networks," in *Proc. IEEE/CVF Conf. Comput. Vis. Pattern Recognit.*, Jun. 2018, pp. 7132–7141.
- [24] D. B. Mulindwa and S. Du, "An n-sigmoid activation function to improve the squeeze-and-excitation for 2D and 3D deep networks," *Electronics*, vol. 12, no. 4, p. 911, Feb. 2023.
- [25] V. Vapnik and V. Vapnik, *Statistical Learning Theory*, vol. 1. New York, NY, USA: Wiley, 1998.
- [26] C. Cortes and V. Vapnik, "Support-vector networks," *Mach. Learn.*, vol. 20, no. 3, pp. 273–297, 1995.
- [27] F. Melgani and L. Bruzzone, "Classification of hyperspectral remote sensing images with support vector machines," *IEEE Trans. Geosci. Remote Sens.*, vol. 42, no. 8, pp. 1778–1790, Aug. 2004.
- [28] O. Daanouni, B. Cherradi, and A. Tmiri, "Self-attention mechanism for diabetic retinopathy detection," in *Emerging Trends in ICT for Sustainable Development*. Berlin, Germany: Springer, 2021, pp. 79–88.
- [29] D. P. Kingma and J. Ba, "Adam: A method for stochastic optimization," 2014, *arXiv:1412.6980*.



**ASMAA MOHAMED** received the bachelor's degree in computer science, in 2016. She is currently a Teaching Assistant with the Higher Institute for Management Sciences, Belqas, Egypt. Her current research interests include artificial intelligence, data analysis, and image processing.

<sup>6</sup>[https://github.com/AhmedAAkl/vermicomposit\\_stages\\_prediction](https://github.com/AhmedAAkl/vermicomposit_stages_prediction)



**AHMED A. AKL** received the master’s degree in computer science from Zagazig University, Egypt, in 2019. He is currently an Assistant Lecturer with the Faculty of Computer and Information, Damanhour University, Egypt. He has more than five years of experience in machine learning and data science. His research interests include machine learning, hyperparameter optimization, computer vision, natural language processing, and deep learning.



**AHMAD SALAH** received the master’s degree in CS from Ain Shams University, Cairo, Egypt, and the Ph.D. degree in computer science from Hunan University, China, in 2014. He is currently an Associate Professor of computer science with Zagazig University, Egypt. He has published more than 50 articles in international peer-reviewed journals, such as *IEEE TRANSACTIONS ON PARALLEL AND DISTRIBUTED SYSTEMS* and *IEEE/ACM TRANSACTIONS ON COMPUTATIONAL BIOLOGY BIOINFORMATICS*, and *ACM Transactions on Parallel Computing*. His current research interests include parallel computing, computational biology, and machine learning.



**M. M. BADR** received the M.Sc. and Ph.D. degrees from the Department of Agricultural Engineering, Faculty of Agriculture, Zagazig University, in 2005 and 2009, respectively. He has published several peer-reviewed articles. His research interests include thermodynamics, heat transfer, renewable energy, electrical engineering, internal combustion engines, farm tractors, and farm energies and powers.



**KHALIL AL RUQEISHI** received the M.Sc. degree in computer science from Teesside University, in 2007, and the Ph.D. degree in computer science from Aston University, in 2016. His research interests include artificial intelligence and cloud computing.



**AMR M. ABDELATIF** received the Ph.D. degree from the Faculty of Computer Science, Cairo University, in 2016. He is currently a Lecturer with the Faculty of Computer Science, Zagazig University. His research interests include compiler construction, prasers, automata, parallel processing, natural language processing, machine learning, and artificial intelligence.

...